Peer-reviewed version available at *Electronics* **2016**, *5*, 68; doi:10.3390/electronics5040068

Article

A Multi-Slope Sliding-Mode Control Approach for Single-Phase Inverters under Different Loads

Ghazanfar Shahgholian * and Babk Khajeh-Shalaly

Department of Electrical Engineering, Najafabad Branch, Islamic Azad University, Najafabad, Isfahan, Iran; babak.khajeh.sh@gmail.com

* Correspondence: shahgholian@iaun.ac.ir; Tel.: +98-31-42292220

Abstract: In this paper, a new approach to the sliding-mode control of single-phase inverters under linear and non-linear loads is introduced. The main idea behind this approach is to utilize a non-linear, flexible and multi-slope function in controller structure. This non-linear function makes the controller possible to control the inverter by a non-linear multi-slope sliding surface. In general, this sliding surface has two parts with different slopes in each part and the flexibility of the sliding surface makes the multi-slope sliding-mode controller (MSSMC) possible to reduce the total harmonic distortion, to improve the tracking accuracy, and to prevent overshoots leading to undesirable transient-states in output voltage which are occurred when the load current sharply rises. In order to improve the tracking accuracy and to reduce the steady-state error, an integral term of the multi-slope function is also added to the sliding surface. The improved performance of the proposed controller is confirmed by simulations and finally, the results of the proposed approach are compared with a conventional SMC and a SRFPI controller.

Keywords: multi-slope sliding-mode control (MSSMC); single-phase inverter; multi-slope function (MS).

1. Introduction

The single-phase inverters are widely used in various applications, such as uninterruptable power supplies [1,2], power filter [3,4], motor derives [5,6], renewable energy conversion [7,8], and etc. The major requirement of its control system is to achieve a proper ac voltage regulation with fast dynamics response for sudden change at loads, good disturbance rejection and a stringent frequency regulation during transients, all this while retaining almost zero steady-state error under linear and non-linear loads [9].

In order to achieve these requirements, numerous control methods have been proposed in the literature [10,11]. Owing to availability and desired process of implementation, prevalent techniques based on repetitive control [12,13], deadbeat control [14,15], multi-loop regulation strategies [16], neural network methods [17,18], iterative learning control [19], adaptive control method [20], have been introduced recently. Repetitive control has acceptable ability to reject periodic disturbances but slow dynamics, poor tracking accuracy, and inappropriate performance to non-periodic disturbances are the weaknesses of this method.

Deadbeat controller provides fast dynamics performance in direct control of inverters. This method is easy to implementation and appropriate design of this method leads to prevent overshoot and ringing, but suffers from the drawbacks, such as sensitivity to system parameters, uncertainties and loading conditions. Continuous-time control strategies based on sliding-mode control technique have been proposed in [21-25], a discontinuous method has been proposed in [21] and a Lyapunov-Function-Based control strategy is also proposed in [22]. The approach in [23] has proper performance but not desired due to the high inductor's current of the output filter which is used as state variable, and moreover, implementation of its switching function is based on the computation of separate sliding surface for each leg with the associated hardware complexity. The sliding mode controller with linear surface is simple to achieve but due to the single-slope and inflexible sliding surface of this method for all values of error, the proper tracking accuracy and transient-states for different values of the error cannot be achieved. In this control structure, for small slopes of the surface, the

Preprints (www.preprints.org) | NOT PEER-REVIEWED | Posted: 19 July 2016 doi:10.20944/preprints201607.0059.v1

Peer-reviewed version available at Electronics 2016, 5, 68; doi:10.3390/electronics5040068

tracking accuracy is decreased and for large slope of the sliding surface, poor transient-states and large overshoots are generated in output voltage in moments of loading.

It has been shown that the inability of the conventional sliding-mode controller and fast SRFPI controller [24] to achieve high-speed operation in reducing the tracking error and desired transient-states in moments of loading at the same time can be overcome by using the proposed control method without the need for complex algorithms. It is worth mentioning that most of the aforementioned drawbacks occur due to the constant slope of the sliding surface or inflexibility of the control method.

In this paper, a new approach to the sliding mode-control of single-phase inverters is introduced. In this approach, by using a non-linear multi-slope (MS) function, a non-linear sliding surface function is generated. In general, this surface consists of two parts with different slopes and slope of the surface for low and large values of the error are different. Therefore, by utilizing this multi-slope function, a considerable improvement can be achieved in transient-states, tracking accuracy and speed of error reduction. The important consequences of this sliding-mode controller are low total harmonic distortion (THD) under different loading conditions, high-speed performance with desired transient-states with a significant reduction in overshoots in loading moments.

2. System Description

The main structure and power stage of a single-phase voltage source inverter (VSI) which is used in this research, as shown in Fig. 1 consisting of a switching part constructed by insulated-gate bipolar transistor (IGBT) or power Mosfet followed by 2nd or more order LC filter. Load in this case is located in parallel with the capacitor of the filter .In practice, to reduce the ESR effect and current ripple, several low ESR capacitors can be connected in parallel structure for the LC filter and it is worth mentioning that the small size of the filter capacitor is necessary and throughout this paper, the dc-link voltage is assumed to be constant. It can be realized by utilizing large capacitances at the dc-link of the inverter. The parameters of the inverter are given in Table 1. The equations describing the dynamics of the inverter can be obtained as:

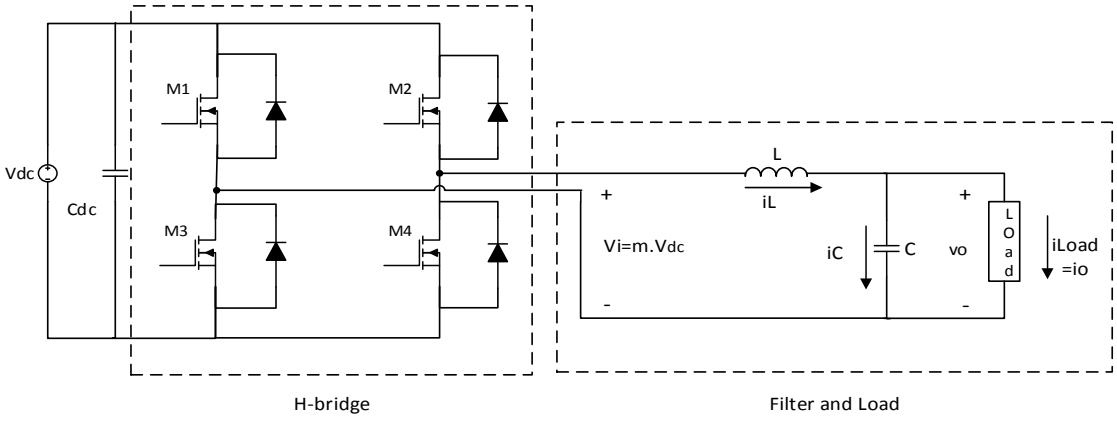

Figure 1. Single-phase inverter

$$v_L = L.\frac{d\,i_L}{dt} = m.V_{dc} - v_o \tag{1}$$

$$i_C = C.\frac{d\,v_c}{dt} = i_L - i_{Load} \tag{2}$$

where m describes the control variable.

Preprints (www.preprints.org) | NOT PEER-REVIEWED | Posted: 19 July 2016 doi:10.20944/preprints201607.0059.v1

Peer-reviewed version available at Electronics 2016, 5, 68; doi:10.3390/electronics5040068

Table 1. Parameters for inverter model

Parameter	Value
Fundamental Frequency, ω	$2\pi 50\ ^{rad}/_{s}$
Output Filter Inductance, L	250μH
Output Filter Capacitance, C	100μF
ESR of the filter Inductance and Capacitor, r_L, r_C	≈ 0
Dc-link voltage	300 V

Considering low ESR capacitors are connected in parallel and the ESRs of the filter capacitor and inductor can be ignored. The state-space equation describing the operation of the system can be written in matrix form, as:

$$\begin{bmatrix} \dot{v}_o \\ \dot{i}_L \end{bmatrix} = \begin{bmatrix} 0 & \frac{1}{C} \\ -\frac{1}{L} & 0 \end{bmatrix} \begin{bmatrix} v_o \\ i_L \end{bmatrix} + \begin{bmatrix} 0 \\ \frac{V_{dc}}{L} \end{bmatrix} m + \begin{bmatrix} -\frac{1}{c} \\ 0 \end{bmatrix} i_{Load} \tag{3}$$

where $m \in \{-1,0,1\}$ is considered as the control input.

Based on (1) and (2), the output voltage error (e(t)) and its derivative (rate of change of the output voltage error) are defined as:

$$e(t) = v_o - v_{oR} \tag{4}$$

$$x_1 = e(t) \tag{5}$$

$$x_2 = \dot{x}_1 = \dot{v}_o - \dot{v}_{oR} \tag{6}$$

$$\dot{x}_2 = D(t) + (m.V_{dc} - x_1).\omega_f^2 \tag{7}$$

where $\dot{x}_1$ denotes the time derivative of x_1, $\omega_f = 1/\sqrt{LC}$, the time-varying term D(t) is considered as a disturbance, and $v_{oR} = V_{Rm}\sin(\omega t)$ is the reference for output voltage. The disturbance term is defined as:

$$D(t) = -v_{oR}.\omega_f^2 - \frac{1}{c}\frac{d(i_L - i_C)}{dt} - \frac{d\dot{v}_{oR}}{dt} \tag{8}$$

The behavior of the system can be expressed by the following state space controllable canonical form:

$$\begin{bmatrix} \dot{x}_1 \\ \dot{x}_2 \end{bmatrix} = \begin{bmatrix} 0 & 1 \\ -\omega_f^2 & 0 \end{bmatrix} \begin{bmatrix} x_1 \\ x_2 \end{bmatrix} + \begin{bmatrix} 0 \\ V_{dc}.\omega_f^2 \end{bmatrix} m + \begin{bmatrix} 0 \\ D(t) \end{bmatrix} \tag{9}$$

Control of single-phase inverters under linear and non-linear loads using the sliding-mode method is well-improved research topic now. In order to achieve a desired control performance in different loading conditions, the controller should have the ability to ensure the low steady-state error in the presence of the inverter model uncertainties as well as other disturbances. In addition to reducing the tracking error in moments of heavy loading, the controller must provide desired transient-states with negligible overshoots in the output voltage during the load current change. Therefore, the previous and single-slope method of sliding-mode control suffers from many problems such as single-slope and inflexible sliding surface, undesirable and poor transient-states in loading moments for sliding-mode controller with large slope of the surface, inability to achieve high-speed response and tracking accuracy simultaneously because of a significant reduction in existence regions for large slope of the surface.

3. Suggested Control Structure

In this section, the problems of conventional SMC will be explained briefly first, then, the novel non-linear function using to produce the multi-slope SMC (MSSMC) will be introduced, after that, its theoretical basis is developed and its coefficients adjustment is explained briefly. Finally, based on a mathematical analysis, the improved performance of the proposed method will be confirmed. Fig. 2 illustrates the suggested control structure, which consists of a MSSMC to regulate the instantaneous output voltage, state generator to provide the system states in order to use in proposed controller and a gate driver part, which is employed to trigger the switches of the VSI.

3.1. Conventional SMC Drawbaks

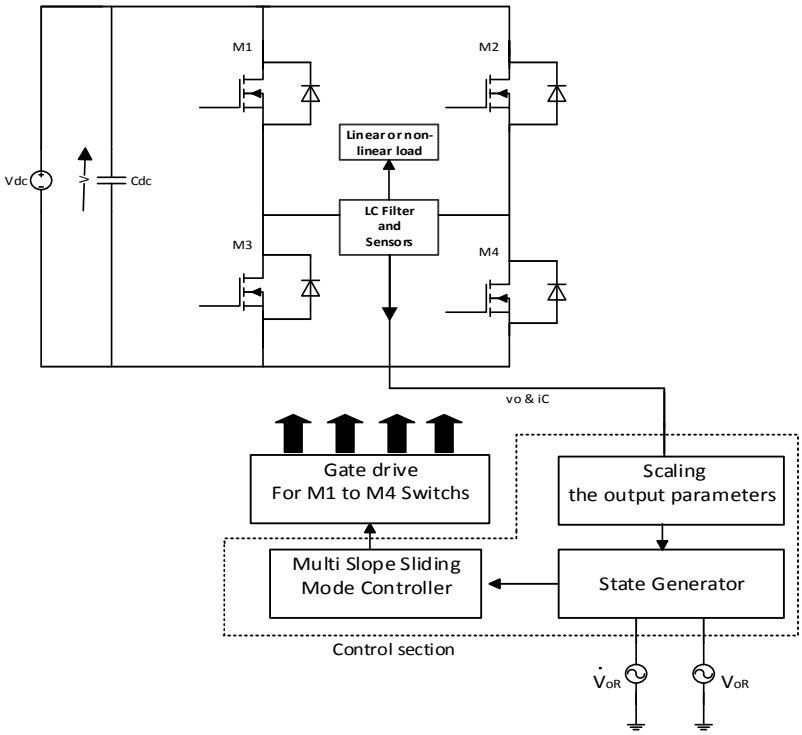

Figure 2. Block diagram of the sliding-mode-controlled inverter with the proposed method

The conventional sliding-mode controller with single-slope sliding surface suffers from the following drawbacks:

- In the conventional sliding function, the integral term is not usually used to accumulate the existing steady-state errors. Even if the integral term is used, lack of flexibility in the integral term still exists for different values of the error. The principal reason behind this problem is the fixed-slope of the integral function for any values of error which can lead to wind-up the integral for different values of the tracking error.

- As mentioned before, one of the most important drawbacks of the conventional sliding-mode controllers is single-slope and inflexible sliding surface. On the other hand, these controllers does not have the ability to achieve both high speed and desired transient-states in loading moment's simultaneously. The surface with small slope leads to a slow response, low tracking accuracy and the surface with large slope leads to a poor transient-state during the load current change. A tradeoff between small and large slopes of the surface, cannot realize both fast response and low THD response without any overshoots in output voltage simultaneously in moments of loading.

3.2. SMC Using Non-Linear Function

In order to overcome the conventional SMC drawbacks, to achieve a desired controller with high speed in reducing the tracking error in moments of loading, and to alleviate steady-state error under

different types of loads without loss of the desired transient response, a flexible sliding surface composed of different terms of a special non-linear function is introduced. It should be noted here that each of these terms is made by a multi-slope non-linear function. Proposed sliding surface with an acceptable approximation consists of two general parts with different slopes, which are shown in Fig. (3-a) with part A and part B. As can be obtained, when the error is generated by load current disturbance, for driving the system states to the sliding surface, a control low is applied to the system. In the sliding mode, the state trajectory reaches to part B of the surface earlier and align the surface goes to the part A with high speed. Therefore, when the error value increases and output voltage drops because of the high current spikes of the load capacitance, the states trajectory hits the part B of the sliding surface first which can lead to a faster reaching mode. It is important to know that in the sliding mode, the VSI will be robust and by changing the slope of the surface, the system dynamics will also change.

3.3. Multi-Slope (MS) Function

The Multi-Slope (MS) function can be described as:

$$Y = MS(x, \alpha, \delta) = (\alpha_1 . x + \alpha_2 . \tanh(\delta . x)) \quad (10)$$

where α1, α2 and δ are adjustable coefficients of the function, which define the general form of the function and it is clear that MS function is a continuous and differentiable function. The variation of slopes in A and B parts and extent of these parts for different values of the multi-slope function coefficients (α1,α2,δ) are shown in Fig. (3-b). This clearly shows that the MS function includes two slopes and for small x values, the slope of the part A and for large value of x, the slope of the part B is more effective in this function.

In order to confirm the effectiveness of the MS function on the controller operation and to demonstrate the performance of the controller, the effectiveness of the proposed MSSMC has been described on a VSI loading behavior.

3.4. MS Function Coefficients Setting

The coefficients of the MS are α1, α2 and δ and to achieve a desired and fast dynamic response with almost negligible overshoot in the output voltage, these coefficients must be adjusted wisely. The task of these coefficients in the MS function structure are as follows:

1. δ coefficient: This coefficient adjusts the slope of the part A and should be positive (δ >0). On the other hand, by changing this coefficient, the gain of the function will be changed for small error values.

2. α1 coefficient: This coefficient is utilized in MS function to adjust the slope of the part B and its effect on slope of the part A is negligible. In principle, this coefficient is utilized to adjust the gain of the MS function for large values of the error.

3. α2 coefficient: This coefficient adjusts the height of the part A. Therefore, by increasing this coefficient, the height of the part A will increase. It is worth mentioning that by increasing the value of this coefficient, low values of error in the input of the function creates more effect in the output of the function.

In general, the MS function is a non-linear function and use of this function in sliding function leads to yield a fast response with a desired transient-state without the need for any complex algorithm. On the other hand, if the coefficients of the MS function are adjusted wisely, a desired sliding surface will be generated which leads to achieve a fast error convergence with a desired transient-state without any overshoots simultaneously.

3.5. Sliding Surface and Stability Considerations

The sliding surface in MSSMC is composed of three MS functions and can be defined as:

$$S = MS(x_1, \alpha_p, \delta_p) + MS(x_2, \alpha_d, \delta_d) + \int MS(x_1, \alpha_i, \delta_i) dt \quad (11)$$

$$S = (\alpha_{p1} x_1 + \alpha_{p2} \tanh(\delta_p . x_1)) + (\alpha_{d1} x_2 + \alpha_{d2} \tanh(\delta_d . x_2)) + \int (\alpha_{i1} . x_1 + \alpha_{i2} \tanh(\delta_i . x_1)) dt \quad (12)$$

In the sliding function, the integral term is added in order to reduce the steady-state error in output voltage and p, i, and d indexes represent the MS function in one of these three terms. When the sliding mode is reached (S=0), we have:

$$\alpha_{d1}\dot{x}_1 + \alpha_{d2}\tanh(\delta_d.\dot{x}_1) = -\alpha_{p1}x_1 - \alpha_{p2}\tanh(\delta_p.x_1) - \int(\alpha_{i1}.x_1 + \alpha_{i2}\tanh(\delta_i.x_1))dt \quad (13)$$

As can be seen, due to the structure of the MS function, the sliding surface is non-linear. It is worth mentioning that for proper performance of the controller, $\alpha_{m1,2}$ must be positive where m can be p, i, and d.

The existence condition must be satisfied for stability of reaching mode as:

$$S\dot{S}<0 \quad (14)$$

We consider the Lyapunov function as $V = 0.5S^2$, and it is clear that for global stability $\dot{V}$ must be negative definite [25]. If this condition is satisfied, the state trajectory will be moved toward the surface and sliding can be preseved until the trajectory reached to the origin. By taking the time derivative of S, substituting (6), (7) into the resulting equation gives:

$$\dot{S} = \alpha_{p_1}.x_2 + \alpha_{p_2}.x_2.\delta_p \sec h^2(\delta_p.x_1) - \alpha_{d1}.\omega_f^2.x_1 + \alpha_{d1}.\omega_f^2.V_{dc}.m + D(t).\alpha_{d1} - \alpha_{d2}.\delta_d.\omega_f^2.x_1.\sec h^2(\delta_d.x_2) + \alpha_{d2}.\delta_d.\omega_f^2.V_{dc}.m.\sec h^2(\delta_d.x_2) + \alpha_{d2}.\delta_d.D(t).\sec h^2(\delta_d.x_2) + \alpha_{i1}.x_1 + \alpha_{i2}.\tanh(\delta_i.x_1). \quad (15)$$

The above equation can be simplified as:

$$\dot{S} = \varepsilon_1(x_1).x_2 - x_1(\varepsilon_2(x_2).\omega_f^2 - \alpha_{i1}) + \varepsilon_2(x_2)(\omega_f^2.V_{dc}.m + D(t)) + \alpha_{i2}.\tanh(\delta_i.x_1). \quad (16)$$

The time derivative of the Lyapunov function is obtained as:

$$\dot{V} = S[\varepsilon_1(x_1).x_2 - x_1(\varepsilon_2(x_2).\omega_f^2 - \alpha_{i1}) + \varepsilon_2(x_2)(\omega_f^2.V_{dc}.m + D(t)) + \alpha_{i2}.\tanh(\delta_i.x_1)]. \quad (17)$$

In (17), $\varepsilon_1(x_1)$ and $\varepsilon_2(x_2)$ are defined as:

$$\varepsilon_1(x_1) = \alpha_{p1} + \delta_p.\alpha_{p2}.\sec h^2(x_1.\delta_p). \quad (18)$$

$$\varepsilon_2(x_2) = \alpha_{d1} + \delta_d.\alpha_{d2}.\sec h^2(x_2.\delta_d). \quad (19)$$

Substitution of m=-sign(S) into (17) yields:

$$\dot{V}(t) = S.\left[\varepsilon_1(x_1).x_2 - x_1(\varepsilon_2(x_2).\omega_f^2 - \alpha_{i1}) - \varepsilon_2(x_2)(\omega_f^2.V_{dc}.\text{sign}(s) - D(t)) + \alpha_{i2}.\tanh(\delta_i.x_1)\right]. \quad (20)$$

$$\dot{V}(t) = |S|.\left\{\text{sign}(s).\left[\varepsilon_1(x_1).x_2 - x_1(\varepsilon_2(x_2).\omega_f^2 - \alpha_{i1}) + \varepsilon_2(x_2)D(t) + \alpha_{i2}.\tanh(\delta_i.x_1)\right] - \varepsilon_2(x_2).\omega_f^2.V_{dc}\right\} \quad (21)$$

It is clear that $\dot{V}(t) < 0$ if :

$$\text{sign}(s).\left[\varepsilon_1(x_1).x_2 - x_1(\varepsilon_2(x_2).\omega_f^2 - \alpha_{i1}) + \varepsilon_2(x_2)D(t) + \alpha_{i2}.\tanh(\delta_i.x_1)\right] < \varepsilon_2(x_2).\omega_f^2.V_{dc} \quad (22)$$

The following inequalities can be obtained from (22):

$$A_1 = -x_2 + x_1\left(\frac{\varepsilon_2(x_2).\omega_f^2 - \alpha_{i1}}{\varepsilon_1(x_1)}\right) - \frac{\varepsilon_2(x_2)}{\varepsilon_1(x_1)}D(t) - \frac{\alpha_{i2}}{\varepsilon_1(x_1)}.\tanh(\delta_i.x_1) - \frac{\varepsilon_2(x_2)}{\varepsilon_1(x_1)}.\omega_f^2.V_{dc} > 0 \quad \text{for } S < 0 \tag{23}$$

$$A_2 = -x_2 + x_1\left(\frac{\varepsilon_2(x_2).\omega_f^2 - \alpha_{i1}}{\varepsilon_1(x_1)}\right) - \frac{\varepsilon_2(x_2)}{\varepsilon_1(x_1)}D(t) - \frac{\alpha_{i2}}{\varepsilon_1(x_1)}.\tanh(\delta_i.x_1) + \frac{\varepsilon_2(x_2)}{\varepsilon_1(x_1)}.\omega_f^2.V_{dc} < 0 \quad \text{for } S > 0 \tag{24}$$

Fig. (3-c) illustrates the regions of existence of the sliding mode. It is clear from (23) and (24) that $A_1=0$ and $A_2=0$ are two lines in the x_1-x_2 plane for the practical values of the inverter parameters. Note that the slopes of these lines are equal which means that these lines are parallel with each other. This slope can be obtained as:

$$s_{L1} = s_{L2} \cong \frac{(\varepsilon_2(0).\omega_f^2 + \alpha_{i1}).\varepsilon_2(x_2)}{\varepsilon_1(0).\varepsilon_2(0)} \cong \frac{\varepsilon_2(x_2).\omega_f^2}{\varepsilon_1(0)} \tag{25}$$

The intersection points of these lines with x_1 and x_2 axes can be obtained from (26)-(29).

$$x_2 = -\frac{\varepsilon_2(D(t) + \omega_f^2.V_{dc})}{\varepsilon_1(0)} \rightarrow \quad A_1 = 0 \text{ with } x_2 - \text{axis} \tag{26}$$

$$x_2 = -\frac{\varepsilon_2(D(t) - \omega_f^2.V_{dc})}{\varepsilon_1(0)} \rightarrow \quad A_2 = 0 \text{ with } x_2 - \text{axis} \tag{27}$$

$$x_1 = \frac{\varepsilon_2(0)(D(t) + \omega_f^2.V_{dc}) + \alpha_{i2}.\tanh(\delta_i.x_1)}{\varepsilon_2(0).\omega_f^2 - \alpha_{i1}} \rightarrow \quad A_1 = 0 \text{ with } x_1 - \text{axis} \tag{28}$$

$$x_1 = \frac{\varepsilon_2(0)(D(t) - \omega_f^2.V_{dc}) + \alpha_{i2}.\tanh(\delta_i.x_1)}{\varepsilon_2(0).\omega_f^2 - \alpha_{i1}} \rightarrow \quad A_2 = 0 \text{ with } x_1 - \text{axis} \tag{29}$$

If the following condition holds:

$$\omega_f^2.\varepsilon_2(0) >> \alpha_{i2}, \alpha_{i1} \tag{30}$$

Equations (28) and (29) can be approximated by:

$$x_1 \cong \frac{(k_1(t))}{\omega_f^2} \rightarrow \quad A_1 = 0 \text{ with } x_1 - \text{axis} \tag{31}$$

$$x_1 \cong \frac{(k_2(t))}{\omega_f^2} \rightarrow \quad A_2 = 0 \text{ with } x_1 - \text{axis} \tag{32}$$

where $k_1(t)$ and $k_2(t)$ are defined as:

$$k_1(t) = D(t) + \omega_f^2.V_{dc} \tag{33}$$

$$k_2(t) = D(t) - \omega_f^2.V_{dc} \tag{34}$$

Due to stability considerations, the existence regions should be kept as large as possible. As can be obtained from (25)- (29), if $\varepsilon_1(0)$ increases to achieve a faster response, this large value of $\varepsilon_1(0)$ causes a reduction in sliding mode existing region which can lead to an overshoot in output voltage. It is clear that for very large value of $\varepsilon_1(0)$, instability can be occurred in the system because of the excessive reduction of the existence regions. In order to increase the sliding mode existing regions and to reduce the overshoots in output voltage for large value of $\varepsilon_1(0)$, It is clear that $\varepsilon_2(0)$ can be adjusted wisely so that the high speed response is yielded and the overshoot is eliminated from the output voltage. Therefore, the distance between the intersection points of the x_2-axis and origin will be increased. In most cases, the following condition holds:

$$\varepsilon_2(0).\omega_f^2 + \alpha_{i1} >> \alpha i_2 \tag{35}$$

Preprints (www.preprints.org) | NOT PEER-REVIEWED | Posted: 19 July 2016 doi:10.20944/preprints201607.0059.v1

Peer-reviewed version available at Electronics 2016, 5, 68; doi:10.3390/electronics5040068

It is clear that the system become unstable with very large $\frac{\varepsilon_1(x_1)}{\varepsilon_2(x_2)}$ value. In most cases, α_{i1} and α_{i2} are chosen so that the following condition holds:

$$\varepsilon_1(x_1) >> (x_1.\alpha_{i1} + \alpha_{i2}.\tanh(\delta_i.x_1)) \quad (36)$$

According to (36) and combination (23) and (24), we obtain:

$$x_2^{-1}.(x_1.\omega_f^2 - D(t) + \omega_f^2.V_{dc}) > \frac{\varepsilon_1(x_1)}{\varepsilon_2(x_2)} > x_2^{-1}.(x_1.\omega_f^2 - D(t) - \omega_f^2.V_{dc}) \quad (37)$$

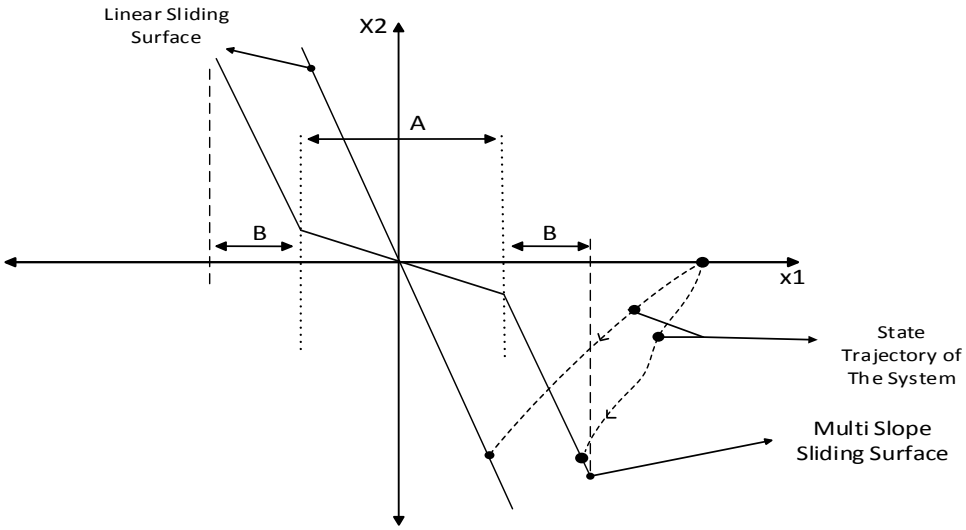

(a) Multi-slope and linear sliding surfaces and trajectory of states during the reaching mode

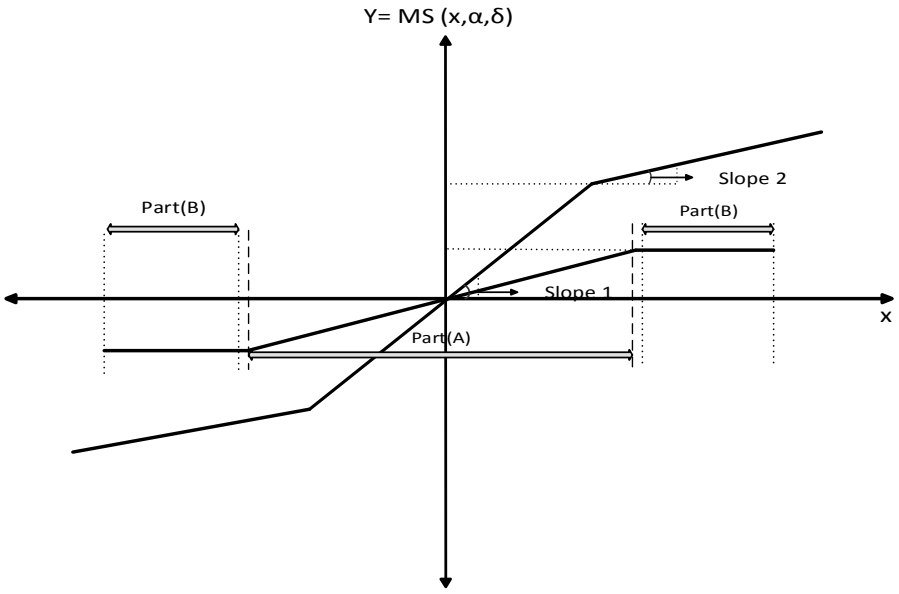

(b) Multi-slope function for different slopes of the part A and part B.

Preprints (www.preprints.org) | NOT PEER-REVIEWED | Posted: 19 July 2016 doi:10.20944/preprints201607.0059.v1

Peer-reviewed version available at Electronics 2016, 5, 68; doi:10.3390/electronics5040068

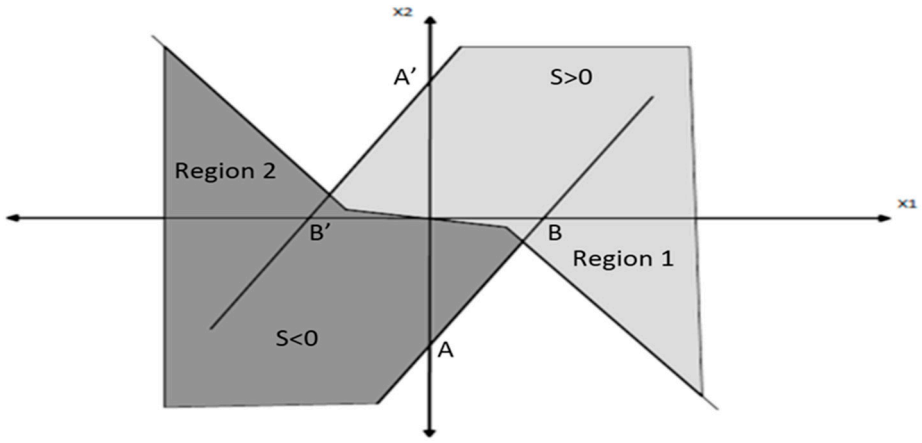

(c) Existence regions of sliding mode in the x_1-x_2 plane

Figure 3. Suggested sliding mod control

an upper bound of $\frac{\varepsilon_1(x_1)}{\varepsilon_2(x_2)}$ can be determined by:

$$x_2^{-1}.(x_1.\omega_f^2 - k_2(t)) > \frac{\varepsilon_1(x_1)}{\varepsilon_2(x_2)} \quad (38)$$

Clearly, the upper bound does not depend on one parameter and has a flexible and adjustable structure which can lead to a fast response without any overshoots.

4. Simulation Results

In this section, the simulation results of an inverter controlled by proposed multi-slope sliding-mode controller under linear and non-linear loads have been evaluated. Due to limited switching frequency of an inverter, the direct implementation of m=-sign(s) is not possible for a VSI in practice. In order to prevent chattering, operating frequency has to be limited to a finite form by replacing a suitable hysteresis function instead of sign function. It is worth mentioning that the simulations are carried out using the Sim-Power-Systems toolbox of Simulink. Fig. (4-a) shows the output voltages for an inverter controlled by proposed MSSMC and a fast controller with high performance proposed in [26]. As can be obtained, both of them are adjusted to generate high speed response with a very low voltage ripple in output voltage. It is clear that, MSSMC leads to an output voltage without any overshoot and Fig. (4-b), shows a larger view of this figure in the loading moment. The simulation results of the proposed controller are obtained when the controller coefficients are chosen as:

$\alpha_{p1}=3\times10^{+6}$, $\alpha_{p2}=4\times10^{+5}$, $\alpha_{d1}=30$, $\alpha_{d2}=6\times10^{+6}$, $\alpha_{i1}=2\times10^{+5}$, $\alpha_{i2}=6\times10^{+5}$, $\delta_p=4000$, $\delta_d=101000$, $\delta_i=6\times10^{+3}$

By utilizing these coefficients, the system response is fast with a negligible overshoot. Fig. (5-a) illustrates the simulated waveforms of output voltage and load current for a resistive load (R=3Ω). As can be seen, the regulation of the output voltage is preserved and the output THD is 0.51%. Fig. (5-b) depicts the output voltage and load current waveforms for a nonlinear triac-controlled resistive load (R=3Ω). The load current changes at the peak of the output voltage and as can be observed, the output voltage regulation is fully preserved and the tracking error reduces with high speed and the output voltage THD is limited under 2.69 % for this load. Fig. (6-a) shows the output voltage and sliding function for a nonlinear triac-controlled resistive load case. Because of the structure of m, the sliding function varies between zero and negative or positive value in positive and negative cycles of the output voltage respectively. Fig. (6-b) illustrates that the output voltage remaining

Preprints (www.preprints.org) | NOT PEER-REVIEWED | Posted: 19 July 2016 doi:10.20944/preprints201607.0059.v1

Peer-reviewed version available at Electronics 2016, 5, 68; doi:10.3390/electronics5040068

constant when a sudden change occurs in the load resistance (at t =7ms) and confirms that the MSSMC has good robustness against the load disturbances.

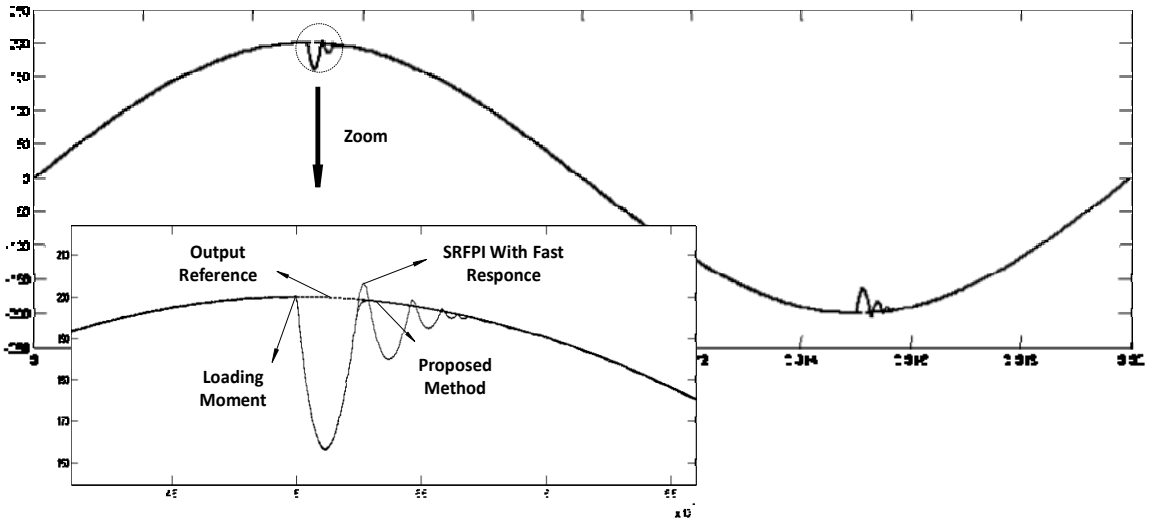

(a) Output voltages of the inverter controlled by fast controller and proposed MSSMC

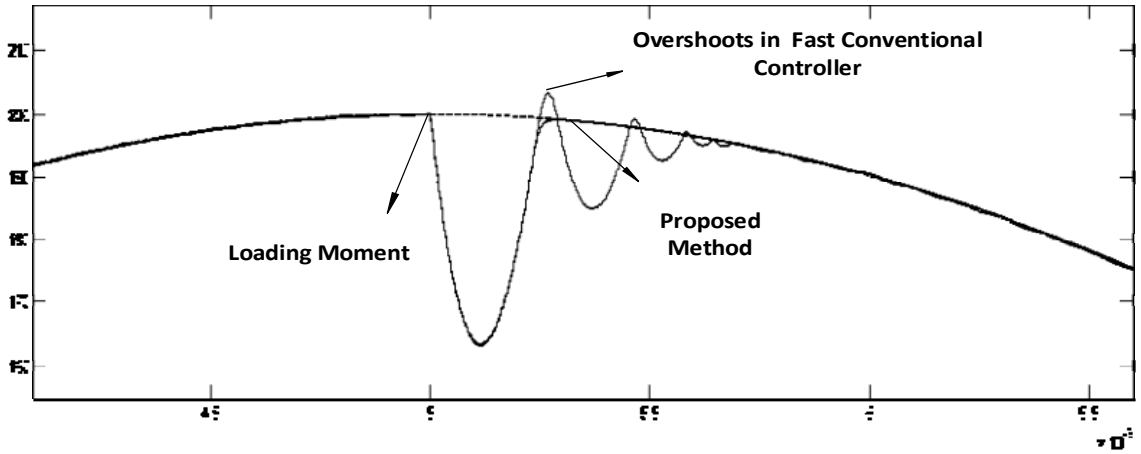

(b) Output voltages of the inverter controlled by proposed MSSMC and a fast controller when loading is performed at the peak of the output voltage

Figure 4. Output voltage of the inverter

Fig. (7-a) shows the output voltage and load current for a bridge rectifier having 10Ω in parallel with a 700μF at the output of the bridge. Output voltage THD for this case was obtained as 0.51%. The output voltage and the sliding function for this bridge rectifier load is shown in Fig. (7-b). Fig. (7-c) depicts the state trajectories of the inverter controlled with proposed and conventional sliding mode controller. It is obvious that the response of the output voltage can be made faster and the output voltage drop (x_1 value) can be reduced by using the proposed MSSMC method. When the current disturbance occurs and the trajectory moves toward the surface, the reaching mode can be reached faster than the conventional SMC because of the improved surface structure.

Fig. (7-d) shows a comparison between the proposed and conventional SMC with the same reaching time. As can be obtained, in both cases, the trajectories reach to each other at the point A, but as can be seen, the drop of the output voltage for the inverter which is controlled by proposed method is lower than the conventional

Preprints (www.preprints.org) | NOT PEER-REVIEWED | Posted: 19 July 2016 doi:10.20944/preprints201607.0059.v1

Peer-reviewed version available at Electronics 2016, 5, 68; doi:10.3390/electronics5040068

SMC. Fig. 8 shows the output voltage spectrum obtained by simulation and it is clear that the magnitude of the output voltage fundamental component is very larger than other components under non-linear load.

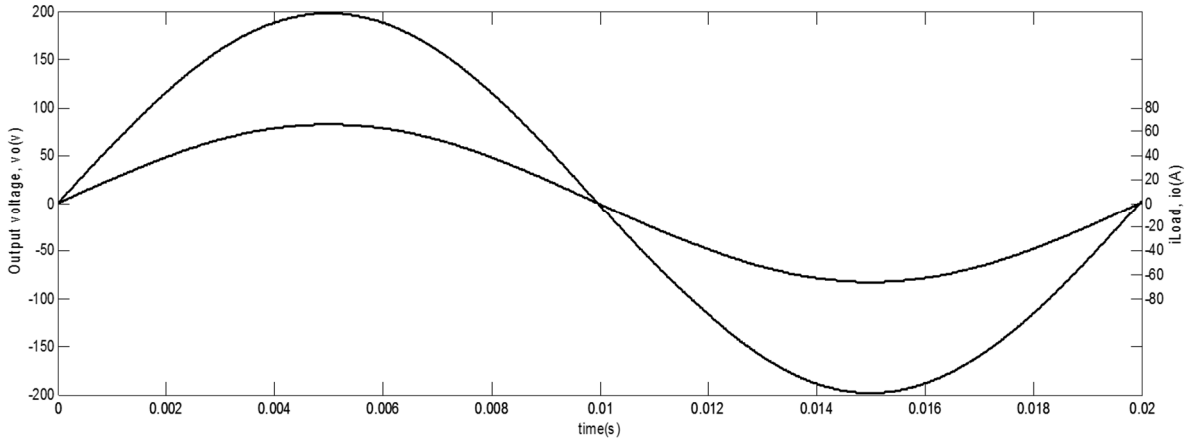

(a) Output voltage and load current waveforms for a resistive load

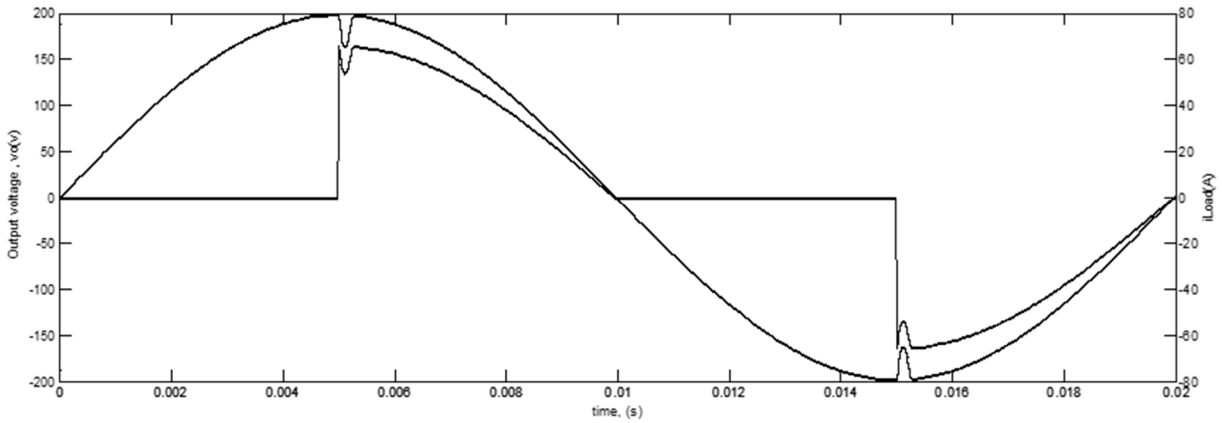

(b) Simulated waveforms of v_o and i_{Load} for a triac-controlled resistive load

Figure 5. Simulation results for a resistive load

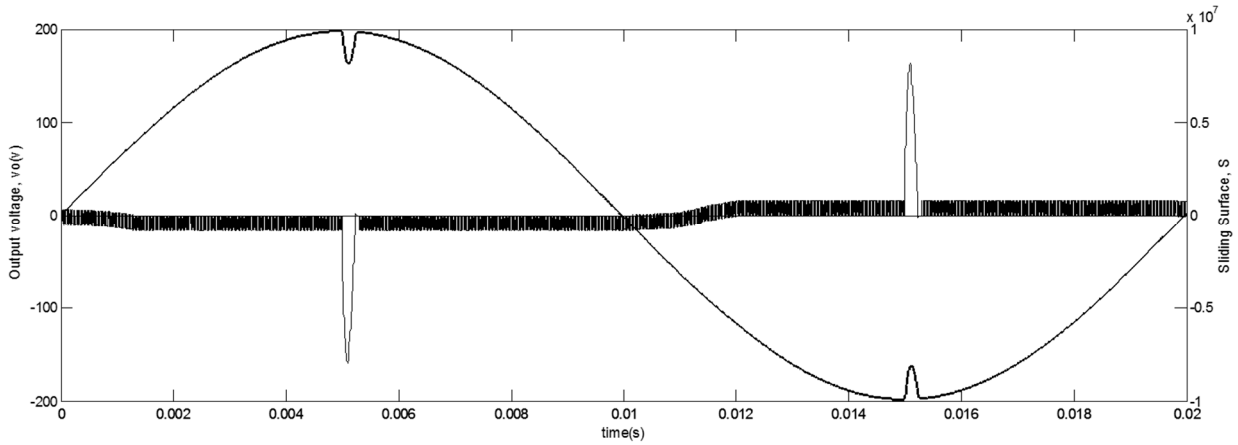

(a) Output voltage and sliding function for a triac-controlled-resistive load

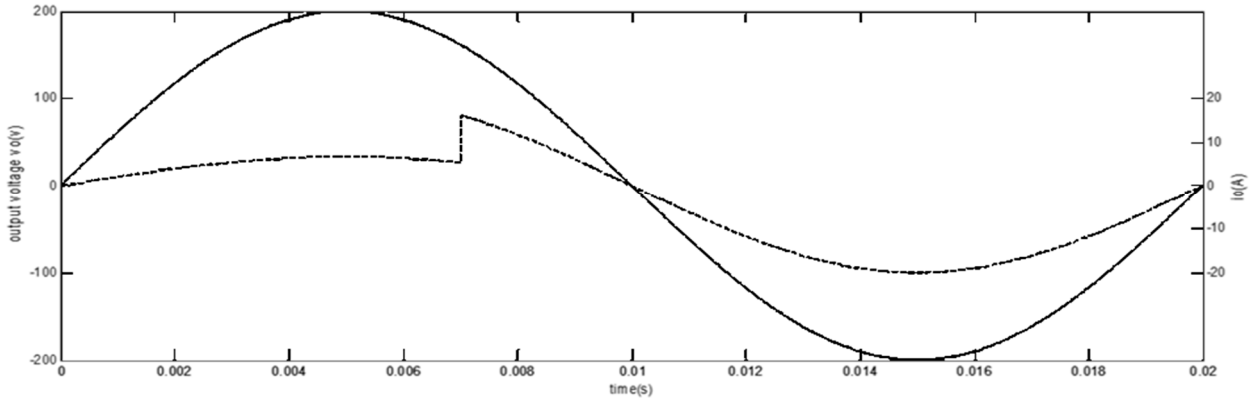

(b) Output voltage and load current for a dynamic change in the load resistance

Figure 6. Output voltage for resistive load

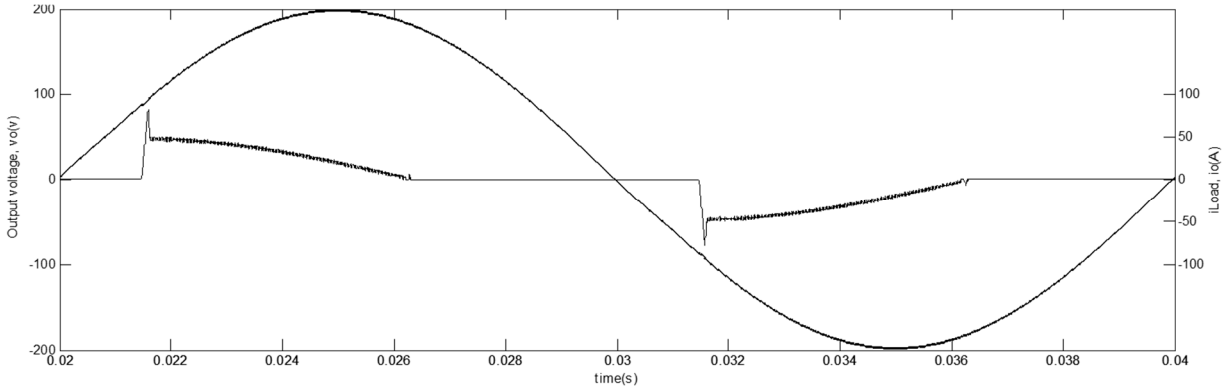

(a) Output voltage and load current for a bridge-rectifier load for the inverter controlled by MSSMC

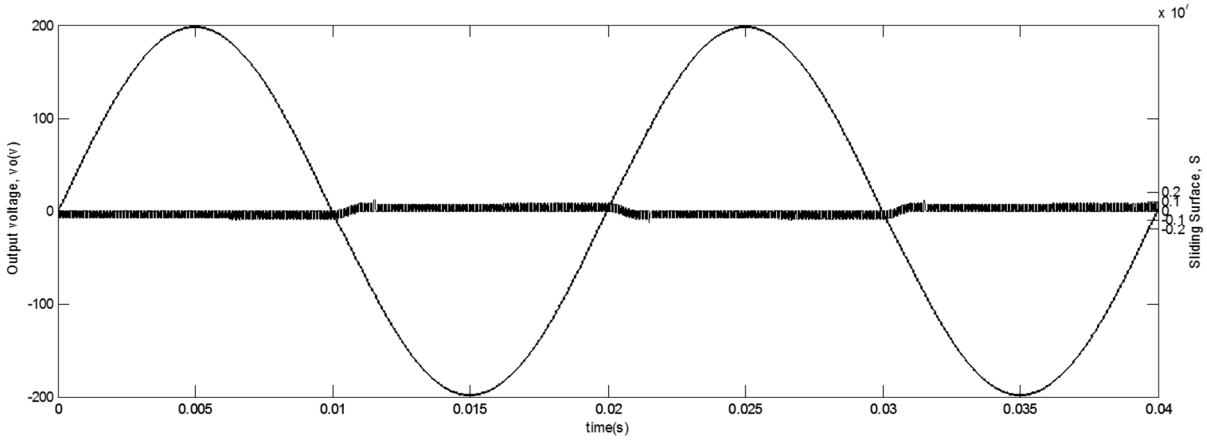

(b) Simulated results of output voltage and sliding function for a diode rectifier load

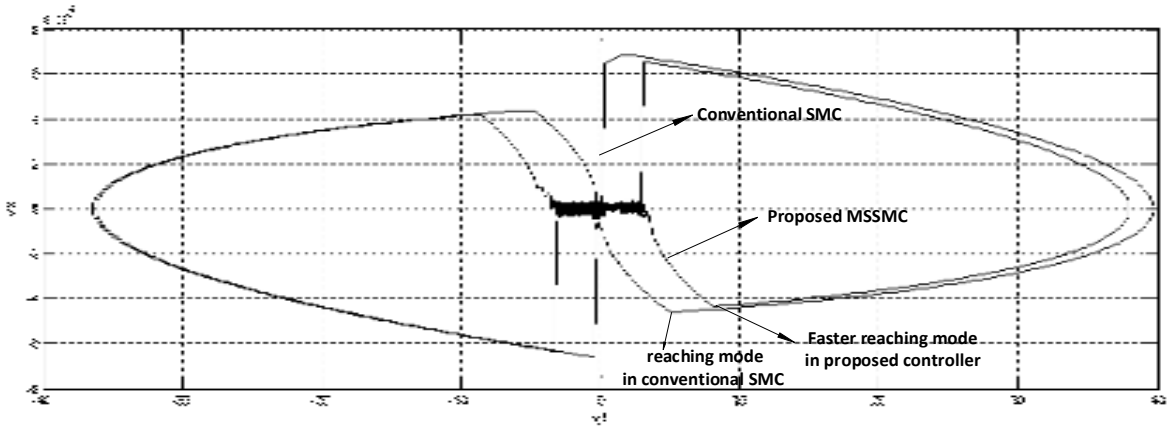

(c) State trajectorys in the phase plane obtained by conventional and proposed controller

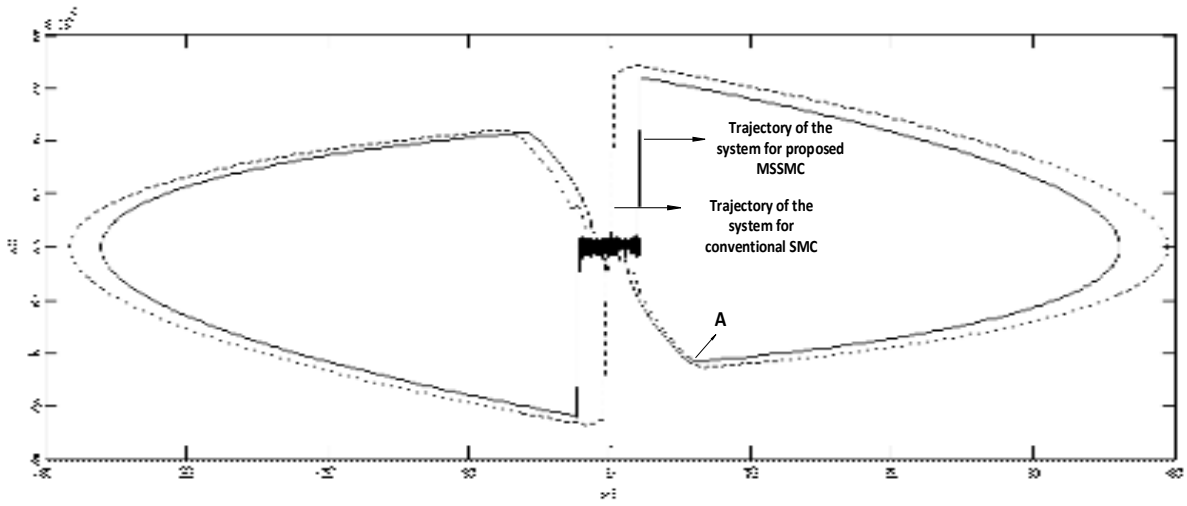

(d) State trajectories in the phase plane obtained by conventional and proposed SMC controller

Figure 7. Simulation results for nonlinear load

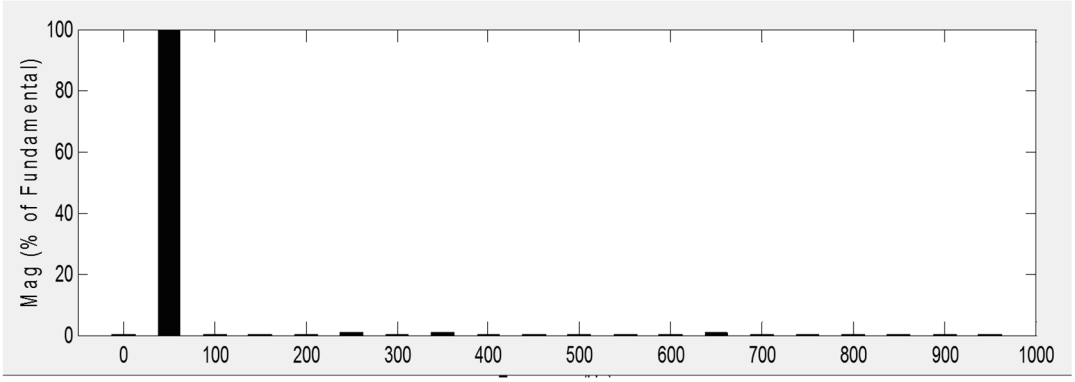

Figure 8. The spectrum of the output voltage under the triac-controlled resistive load

The simulation results of proposed MSSMC controller in comparison with conventional SMC and a fast controller [31] are evaluated in the same inverter topology and loading conditions for nonlinear load case. Table 2 summarizes the output voltage harmonic analysis in three methods for the Triac-controlled resistive load case. As can be obtained, three techniques can supply different load types with very small THD in generated voltage

but the proposed technique produced an output voltage with lower harmonic contents than the output voltage produced by the conventional SMC and fast controller under the nonlinear load.

Table 2. THD and harmonics of the output voltage for three control methods

Comparison Category	Proposed Method in [26] k_p=15, k_i=50, k=30	Proposed MSSMC	Single slope SMC ($s=\lambda x_1+x_2$), λ=60000
THD (%) for nonlinear load case	2.85	2.69	3.10
Output Voltage Fundamental (v)	198.5	196.7	198.5
2nd harmonic (% of fundamental)	0.04	0.08	0.02
3rd harmonic (% of fundamental)	0.45	0.18	0.65
4th harmonic (% of fundamental)	0.03	0.07	0.02
5th harmonic (% of fundamental)	0.65	0.74	0.68
Robustness	Good	Very good	Very good

5. Conclusions

In order to achieve an accurate and desired performance of single-phase sinusoidal inverter under different load types, a new approach to the sliding-mode controller is introduced in this paper. In this controller by using a non-linear multi-slope function (MS), a multi-slope sliding surface is made consisting of two parts with different slopes. Slope of the surface in each part can be changed by setting the coefficients of the multi-slope function. It is shown that in this approach, the speed of the controller to reduce the tracking error in moments of heavy loading can be increased and fast transient-states can be obtained without any overshoot. Therefore, proposed approach leads to achieve a high-speed response with a desired transient-states when the load current change and under a highly nonlinear load. Finally, the performance of the proposed control strategy has been confirmed through simulations.

Author Contributions: Ghazanfar Shahgholian supervised the progress of research. Babk Khajeh-Shalaly conducted the literature review. Both authors reviewed and polished the manuscript

Conflicts of Interest: The authors declare no conflict of interest.

References

1. J. Merry Geisa, M. Rajaram, "Selective elimination of harmonic contents in an uninterruptible power supply: an enhanced adaptive hybrid technique", *IET Power Electronics*, **2012**, Vol. 5, No. 8, pp. 1527-1534 (doi:10.1049 /iet-pel.2011.0472).
2. S. Roy,L. Umanand, "Magnetic arm-switch-based three-phase series-shunt compensated quality ac power supply", *IET Electric Power Applications*, **2012**, Vol. 6, No. 2, pp. 91-100 (doi:10.1049/iet-epa.2010.0294).
3. J. Tian, Q. Chen, B. Xie, "Series hybrid active power filter based on controllable harmonic impedance", *IET Power Electronics*, **2012**, Vol. 5, No. 1, pp. 142-148 (doi: 10.1049/iet-pel.2011.0003).
4. A.M. Massoud, S.J. Finney, A. Cruden, B.W. Williams, "Mapped phase-shifted space vector modulation for multi-level voltage-source inverters", *IET Electric Power Applications*, **2007**, Vol. 1, No. 4, pp. 622-636 (doi:10.1049/iet-epa:20060273).

5. K. R.Sekhar,S. Srinivas, "Discontinuous decoupled PWMs for reduced current ripple in a dual two-level inverter fed open-end winding induction motor drive", *IEEE Trans. on Power Electronics*, **2012**, Vol. 28, No. 5, pp. 2493-2502 (doi:10.1109/TPEL.2012.2215344).
6. Y. Chen, T.H. Liu, N.M. Cuong, "Implementation of sensorless DC-link capacitorless inverter-based interior permanent magnet synchronous motor drive via measuring switching-state current ripples", *IET Electric Power Applications*, **2016**, Vol.10, No. 3, pp. 197-207, March 2016 (doi:10.1049/iet-epa.2015.0303).
7. B.R. Lin, J.Y. Dong, "New zero-voltage switching DC-DC converter for renewable energy conversion systems", *IET Power Electronics*, **2012**, Vol. 5, No. 4, pp. 393-400 (doi:10.1049/iet-pel.2011.0002).
8. E. Pouresmaeil, D. Montesinos-Miracle, O. Gomis-Bellmunt, "Control scheme of three-level NPC inverter for integration of renewable energy resources into AC grid", *IEEE Systems Journal*, **2012**, Vol. 6, No. 2, pp. 242–253 (doi:10.1109/JSYST.2011.2162922).
9. J. Faiz, Gh. Shahgholian, M. Ehsan, "Stability analysis and simulation of a single-phase voltage source UPS inverter with two-stage cascade output filter", *European Trans. on Electrical Power*, **2008**, Vol. 18, No. 1, pp. 29-49 (doi:10.1002/etep 160).
10. Gh. Shahgholian, J. Faiz, M. Jabbari, "Voltage control techniques in uninterruptible power supply inverters: A review", *International Review of Electrical Engineering*, **2011**, Vol. 6, No. 4, pp. 1531-1542, Aug. 2011.
11. J. Faiz, G. Shahgholian, "Modeling and simulation of a three-phase inverter with rectifier-type nonlinear loads", *Armenian Journal of Physics*, **2009**, Vol. 2, No. 4, pp.307-316.
12. G. Escobar, A.A. Valdez, J. Leyva-Ramos, P. Mattavelli, "Repetitive rased controller for a UPS inverter to compensate unbalance and harmonic distortion", *IEEE Trans. on Industrial Electronics*, **2007**, Vol. 54, No. 1, pp. 504–510 (doi: 10.1109/TIE.2006.888803).
13. B. Zhang, D. Wang, K. Zhou, Y. Wang, "Linear phase lead compensation repetitive control of a CVCF PWM inverter", *IEEE Trans. on Industrial Electronics*, **2008**, Vol. 55, No. 4, pp. 1595-1602 (doi:10.1109/TIE .2008.917105).
14. C. Wang,B.T. Ooi, "Incorporating deadbeat and low-frequency harmonic elimination in modular multilevel converters", *IET Gener. Transm. Distrib.*, **2015**, Vol. 9, No. 4, pp. 369-378 (doi: 10.1049/iet-gtd.2014.0429).
15. P. Mattavelli, "An improved deadbeat control for UPS using disturbance observer", *IEEE Trans. on Industrial Electronics*, **2005**, Vol. 52, No. 1, pp. 206–211 (doi:10.1109/TIE.2004.837912).
16. P.C. Loh, M.J. Newman, D.N. Zmood, D.G. Holmes, "A comparative analysis of multi-loop voltage regulation strategies for single and three-phase UPS systems", *IEEE Trans. on Power Electronics*, **2003**, Vol. 18, No. 5, pp. 1176–1185 (doi: 10.1109/TPEL.2003.816199).
17. X. Sun, M. H. L. Chow, F. H. F. Leung, D. Xu, Y. Wang, Y.S. Lee, "Analogue implementation of a neural network controller for UPS inverter applications", *IEEE Trans. on Power Electronics*, **2002**, Vol. 17, No. 3, pp. 305-313 (doi: 10.1109/TPEL.2002.1004238).
18. K.W.E. Cheng, H.Y. Wang, D. Sutanto,"Adaptive directive neural network control for three-phase AC/DC PWM converter", *Proceeding Electrical Power Applications*, **2001**, Vol. 148, No. 5, pp. 425–430 (doi: 10.1049/ip-epa:20010564).
19. H. Deng, R. Oruganti, D. Srinivasan, "Analysis and design of iterative learning control strategies for UPS inverters", *IEEE Trans. on Industrial Electronics*, **2007**, Vol. 54, No. 3, pp. 1739–1751 (doi: 10.1109/TIE.2007. 894701).
20. G. Escobar, P. Mattavelli, A. M. Stankovic, A. A. Valdez, J. M. Ramos, "An adaptive control for UPS to compensate unbalance and harmonic distortion using a combined capacitor/load current sensing", *IEEE Trans. on Industrial Electronics*, **2007**, Vol. 54, No. 2, pp. 839–847 (doi: 10.1109/TIE.2007.891998).
21. S.H. Chang, P.Y. Chen, Y.H. Ting, S.W. Hung, "Robust current control-based sliding mode control with simple uncertainties estimation in permanent magnet synchronous motor drive systems", *IET Electric Power Applications*, **2010**, Vol. 4, No. 6, pp. 441-450 (doi:10.1049/iet-epa.2009.0146).
22. H. Komurcugil et al "Sliding-mode control for single-phase grid connected LCL-filtered VSI with double band hysteresis control scheme", *IEEE Trans. on Industrial Electronics*, **2016**, Vol. 63, No. 2, pp. 864-873 (doi: 10.1109/TIE.2015.2477486).
23. H. Komurcugil, "Nonsingular terminal sliding mode control of DC-DC buck converters", *Control Engineering Practice*, **2013**, Vol. 21, pp. 321-332.
24. X. Hao, X. Yang, T. Liu, L. Huang, W. Chen, "A sliding-mode controller with multiresonant sliding surface for single-phase grid-connected VSI with an LCL filter", *IEEE Trans. on Power Electronics*, **2013**, Vol. 28, No. 5, pp. 2259–2268 (doi: 10.1109/TPEL.2012.2218133).

25. A. Susperregui, M.I. Martinez, I. Zubia, G. Tapia, "Design and tuning of fixed-switching-frequency second-order sliding-mode controller for doubly fed induction generator power control", *IET Electric Power Applications*, **2012**, Vol. 6, No. 9, pp. 696-706 (doi:10.1049/iet-epa.2011.0358).
26. T. L. Tai, J. S. Chen, "UPS inverter design using discrete-time sliding-mode control scheme", *IEEE Trans. on Industrial Electronics*, **2002**, Vol. 49, No. 1, pp. 67-75 (doi:10.1109/41.982250).
27. H.Komurcugil et al. "An extended Lyapunov-function-based control strategy for single-phase UPS inverters", *IEEE Trans. on Power Electronics*, **2015**, Vol. 30, No. 7, pp. 3976-3983 (doi: 10.1109/TPEL.2014. 2347396).
28. S.J Chiang, T.L Tie, T.S Lee, "Variable structure control of UPS inverters", *IEE Proceeding Electrical Power Applications*, **1998**, Vol. 145, pp. 559-567 (doi: 10.1049/ip-epa:19982334).
29. S. Golestan, M. Monfared, J.M. Guerrero, M. Joorabian, "A D-Q synchronous frame controller for single-phase inverters", *Proceeding of the IEEE/PEDSTC*, **2011**, pp. 317-323, Tehran, Iran (10.1109/PEDSTC.2011 .5742439).
30. H. Komurcugil, "Rotating-sliding-line-based sliding-mode control for single-phase UPS inverters", *IEEE Trans. on Industrial Electronics*, **2012**, Vol. 59, No. 10, pp. 3719–3726 (doi: 10.1109/TIE.2011.2159354).
31. M. Monfared, S. Golestan, J. M. Guerrero, "Analysis, design, and experimental verification of a synchronous reference frame voltage control for single-phase inverters", *IEEE Trans. on Industrial Electronics*, **2014**, Vol. 61, No. 1, pp. 258-269 (doi: 10.1109/TIE.2013.2238878).